Biogeosciences Discuss., 6, 5339–5372, 2009
www.biogeosciences-discuss.net/6/5339/2009/

Biogeosciences Discussions

Biogeosciences Discussions is the access reviewed discussion forum of *Biogeosciences*

Carbon fixation prediction during a bloom of *Emiliania huxleyi* is highly sensitive to the assumed regulation mechanism

O. Bernard[1,2], **A. Sciandra**[2], **and S. Rabouille**[2]

[1]COMORE-INRIA, BP 93, 06902 Sophia-Antipolis Cedex, France
[2]LOV, UMR 7093, Station Zoologique, BP 28, 06234, Villefranche-sur-mer, France

Received: 1 April 2009 – Accepted: 5 May 2009 – Published: 28 May 2009

Correspondence to: O. Bernard (olivier.bernard@inria.fr)

Published by Copernicus Publications on behalf of the European Geosciences Union.

Abstract

Large scale precipitation of calcium carbonate in the oceans by coccolithophorids plays an important role in carbon sequestration. However, there is a controversy on the effect of an increase in atmospheric CO_2 concentration on both calcification and photosynthesis of coccolithophorids. Indeed recent experiments, performed under nitrogen limitation, revealed that the associated fluxes may be slowed down, while other authors claim the reverse. We designed models to account for various scenarii of calcification and photosynthesis regulation in chemostat cultures of *Emiliania huxleyi*, based on different hypotheses on the regulation mechanism. These models consider that either carbon dioxide, bicarbonate, carbonate or calcite saturation state (Ω) is the regulating factor. All were calibrated to predict the same carbon fixation rate in nowadays pCO_2, but they turn out to respond differently to an increase in CO_2 concentration. Thus, using the four possible models, we simulated a large bloom of *Emiliania huxleyi*. It results that models assuming a regulation by CO_3^{2-} or Ω predicted much higher carbon fluxes. The response when considering a doubled pCO_2 was different and models controlled by CO_2 or HCO_3^- led to increased carbon fluxes. In addition, the variability between the various scenarii proved to be in the same order of magnitude than the response to pCO_2 increase. These sharp discrepancies reveal the consequences of model assumptions on the simulation outcome.

1 Introduction

Coccolithophorids play an important role in CO_2 trapping (Frankignoulle et al., 1994), since they transform dissolved inorganic carbon (DIC) into respectively particulate organic and inorganic matter which, being denser than seawater, sink towards the ocean floor. Such export of both particulate organic carbon (POC) (see Eq. 1) and particulate inorganic carbon (PIC) (see Eq. 2), operated by the biological pump from the surface ocean layers, constitutes a carbon sink to the deep ocean on a geological scale

BGD

6, 5339–5372, 2009

(Klepper et al., 1994; Falkowski, 1997).

$$6CO_2 + 12H_2O \longrightarrow C_6H_{12}O_6 + 6O_2 + 6\,H_2O \quad (1)$$

$$Ca^{2+} + 2HCO_3^- \longrightarrow CaCO_3 + CO_2 + H_2O \quad (2)$$

Coccoliths formation thus accounts for nearly 70% of the biogenic carbonate precipitation in the oceans (Houghton et al., 1996). Yet, such structures are relatively sensitive to pH and tend to dissolve when the water becomes too acidic. It is expected that a doubling in pCO_2 will have direct consequences on the ability of these organisms to maintain their growth rate (Riebesell et al., 2000; Sciandra et al., 2003). As a corollary, acidification of the oceans due to increase in atmospheric pCO_2 (Orr et al., 2005) could jeopardize their role as a CO_2 pump.

Hence, how coccolithophorids may respond to shifts in global pCO_2 is a critical question to be answered. However, if the chemical phenomena driving the coccoliths dissolution are well known, the effects of pCO_2 changes, whether on photosynthesis or on calcification, are still subject to intense debates (Paasche, 2002; Berry et al., 2002; Riebesell et al., 2008). Contradictory observations were made in batch experiments, where doubling pCO_2 either led to a decrease (Riebesell et al., 2000) or an increase (Iglesias-Rodriguez et al., 2008) in calcification in *Emiliana huxleyi* while photosynthesis was enhanced. Continuous cultures experiments in chemostats supported the hypothesis that both photosynthesis and calcification decrease (Sciandra et al., 2003), while photosynthesis was increased in a study with non calcifying strain (Leonardos and Geider, 2005).

Since the pioneer works of Paasche (1968) the functional relationship between calcification and photosynthesis continues to cause intense research leading to contradictory results for several reasons (see Paasche, 2002, for a compilation). The nature of the physiological coupling between photosynthesis and calcification is far from being completely elucidated (Berry et al., 2002). On the one hand, the functional link is not essential since (i) non calcifying strains of *E. huxleyi* exist, and (ii) the loss of this function in normally calcifying strains is not necessarily accompanied by a deficient growth.

On the other hand, several experiments have shown that photosynthesis can directly or indirectly use the CO_2 produced by calcification; this is an advantage for *E. huxleyi* whose affinity for dissolved CO_2 in seawater is low (Buitenhuis et al., 1999). Thirdly, the kind of transport (active vs. passive) and the C substrates (CO_2 vs. HCO_3^--) implied in the uptake of DIC are still subject to debate. It is only recently that carbon concentration mechanisms (CCM), implying intra or extracellular carbonic anhydrase enzymes, were detected in *E. huxleyi* (Nimer and Merrett, 1996). Nevertheless the CCM efficiency in *E. huxleyi* seems low compared to others species (Rost et al., 2003, 2006).

Considering the chemical equations for photosynthesis (1) and calcification (2), a classical Michaelis-Menten based kinetics for growth could be proposed, involving, respectively CO_2 and HCO_3^-. However, such representation follows the dogmatic assumption that photosynthesis is regulated by the CO_2 concentration only, and calcification is regulated by HCO_3^-only. Yet, Riebesell et al. (2000) and Sciandra et al. (2003) indirectly demonstrated that HCO_3^- could not regulate calcification: their experiments showed that an increase in HCO_3^- led to a decrease in the calcification rate. These contradictory experimental results spurred Bernard et al. (2008) to propose and analyse 12 models based on different assumptions as for the inorganic carbon species regulating calcification and photosynthesis, taken among CO_2, HCO_3^- and CO_3^{2-}. Model simulations suggested that only the models where carbonate ion regulates calcification could reproduce the decrease in calcification rate after a pCO_2 doubling, hence refuting the general assumption of a regulation by HCO_3^-. Indeed, CO_3^{2-} is the only species whose concentration decreases when pCO_2 increases. This hypothesis is corroborated by Merico et al. (2006) who suggest that the condition of high CO_3^{2-} can be considered as a crucial ecological factor for the success of *E. huxleyi*. However, this hypothesis needs clarification from a biological point of view. As stated by Riebesell (2004), carbonate saturation state may exert a stronger control on calcification than any of the other possible candidates, e.g. pH, CO_2, or CO_3^{2-} concentrations. We thus considered here a fourth regulating variable, namely the calcite saturation state Ω, and we introduce a new model, with Ω acting as a regulating factor. The underlying phytoplankton growth

model, based on the representation of a cell quota, is a Droop-like model (Droop, 1968; Burmaster, 1979; Droop, 1983) in which we added the dependence to both inorganic carbon and light.

Our goal is to point out how the generic model of (Bernard et al., 2008), successively run with the different regulating factors, can predict significantly different amounts and fluxes of carbon. We simulated the typical situation of an *Emiliania huxleyi* late-Spring bloom, following a diatoms bloom which depleted the inorganic carbon stock (Riebesell et al., 1993). The four versions of the model only differ by their assumption on the factor regulating the inorganic carbon uptake. In this simplified model, we assume that all the chemical and biological concentrations are homogeneous in the mixed layer. The main idea developed throughout this paper is that some transient phenomena can lead to paradoxical effects on the predicted carbon fluxes. Hence we show that, depending on the supposed regulating factor, the exported carbon can vary two-fold. Results also reveal that the fluxes variability, due to the assumed regulating factor, is higher than the influence of a pCO_2 increase, because of the slow transfer rate of inorganic carbon through the atmosphere – seawater interface.

In the following section, we present the biological model of growth and calcification and describe its variants, according to the chemical species regulating the inorganic carbon compartment. We then recall classical modelling theories of the carbonate system dynamics in seawater. The hydrodynamical structure of the water column, in the considered typical situation, is exposed in Sect. 3 and the parameters calibration are detailed in Sect. 4. Section 5 is devoted to model simulations under two environmental conditions, represented by the current pCO_2 and that expected in the end of the 21st century, after a pCO_2 doubling.

2 Modelling growth and calcification of coccolithophorids

2.1 Phytoplankton growth in conditions of nitrogen limitation

Uptake of inorganic nitrogen (nitrate, denoted S_1) by the phytoplanktonic biomass (whose particulate nitrogen concentration is denoted N), can be represented by the following mass flow, where $\rho(.)$ is the nitrate absorption rate:

$$S_1 \xrightarrow{\rho(.)X} N \tag{3}$$

The flux of inorganic carbon into organic biomass X and coccoliths C is associated to a flux of calcium (Ca^{2+}, denoted S_2) and of dissolved inorganic carbon (D), where $\mu(.)$ is the photosynthesis rate:

$$\frac{1-\alpha}{\alpha} S_2 + \frac{1}{\alpha} D \xrightarrow{\mu(.)X} \frac{1-\alpha}{\alpha} C + X \tag{4}$$

Here, for sake of simplicity, we assume that photosynthesis and calcification are coupled (see Bernard et al., 2008, for models where these processes are uncoupled). The constant α represents the proportion of the total up taken DIC which is allocated to photosynthesis.

The next step in the model development is the mathematical expression for both the nitrate absorption rate $\rho(.)$ and the photosynthesis rate μ.

Generally, nitrate uptake is assumed to depend on external nitrate concentration NO_3, following a Michaelis-Menten type equation (Dugdale, 1967):

$$\rho(S_1) = \rho_m S_1 / (S_1 + k_N) \tag{5}$$

The expression of the rate of inorganic carbon acquisition is more tricky; as shown by Droop (1968, 1983), this rate must depend on the internal nitrogen quota Q. However, coccolithophorids photosynthesis and calcification are also sensitive to the DIC concentration, and there is a consensus to admit that CO_2 would be the substrate for

photosynthesis while HCO_3^- would be the substrate for calcification. Therefore the regulation of growth and calcification could theoretically be triggered by CO_2 or HCO_3^-. In addition, we examined the possibility that CO_3^{2-} is involved in the regulation of inorganic carbon acquisition, as suggested by recent works (Bernard et al., 2008). Last, we also consider that availability of calcium can potentially regulate photosynthesis and calcification. In this last hypothesis, $\mu(.)$ is a function of Ω, the saturation state of calcite ($CaCO_3$):

$$\Omega = \frac{[Ca^{2+}][CO_3^{2-}]}{K_{sp}} \tag{6}$$

where the solubility constant yields $K_{sp}=5.15\,10^{-7}\,mol^2\,L^{-2}$.

As a consequence, in the sequel we examine four possible models that only differ by the regulation mechanism of inorganic carbon acquisition:

- CO_2 is the regulating species, and thus $\mu(Q,CO_2)$ is an increasing function of both Q and CO_2.
- HCO_3^- is the regulating species, and thus $\mu(Q, HCO_3^-)$ is an increasing function of both Q and HCO_3^-.
- CO_3^{2-} is the regulating species, and thus $\mu(Q,CO_3^{2-})$ is an increasing function of both Q and CO_3^{2-}.
- Ω is the regulating species, and thus $\mu(Q, \Omega)$ is an increasing function of both Q and Ω.

To keep a general denomination, we denote $\mu_p(Q,D_p)$ the growth rate, where, depending on the model $\mathcal{M}_p$, D_p is chosen among CO_2, HCO_3^-, CO_3^{2-} and Ω.

The analytical expression of $\mu_p(Q, D_p)$ is then based on the Droop model (Droop, 1968, 1983):

$$\mu(Q, D_p)=\bar{\mu}(I_0)(1-\frac{k_Q}{Q})\frac{D_p}{D_p+k_{D_p}}-R \quad (7)$$

where k_Q and k_{D_p} are, respectively the subsistence quota and the half-saturation constant for the chosen regulating species. The mortality rate R accounts for respiration and grazing losses, and is supposed constant. The maximum hypothetical growth rate at light I is denoted $\bar{\mu}(I)$, and we use the following expression, supported e.g. by Nimer and Merrett (1993):

$$\bar{\mu}(I)=\bar{\mu}\frac{I}{I+K_I} \quad (8)$$

The maximum hypothetical growth rate averaged on the mixed layer is denoted $\bar{\bar{\mu}}(I_0)$. It depends on the incident irradiance I_0.

To compute this term, we take into account the exponential decrease of light with depth. We use the model of Oguz and Merico (2006) assuming that light extinction rate is the sum of a constant rate k_1 (due to the background and suspended material extinction) and of a rate proportional to phytoplanktonic nitrogen N (due to the biomass-specific extinction of the phytoplankton).

$$I(z)=I_0\ \exp(-(k_1+k_2 N)z) \quad (9)$$

The average value of the maximum hypothetical growth rate $\bar{\mu}\frac{I(z)}{I(z)+K_I}$ in the mixed layer of depth L, can then be computed as follows:

$$\bar{\bar{\mu}}(I_0)=\frac{1}{L}\int_0^L \bar{\mu}\frac{I_0\exp(-(k_1+k_2 N)z)}{I_0\exp(-(k_1+k_2 N)z)+K_I}dz \quad (10)$$

a straightforward computation leads to:

$$\bar{\mu}(I_0)=\frac{1}{(k_1+k_2\mathrm{N})\mathrm{L}}\ln\frac{I_0+K_I}{I_0\exp(-(k_1+k_2\mathrm{N})\mathrm{L})+K_I} \quad (11)$$

2.2 Inorganic carbon modelling

In order to compute CO_2, HCO_3^-, CO_3^{2-} and Ω from DIC (D) and Ca^{2+} (S_2), classical equations of the seawater carbonate system must be considered (Zeebe and Wolf-Gladrow, 2003; Millero, 2007).

The carbonate alkalinity (CA) represents the sum of the electric charges carried in the carbonate system:

$$\mathrm{CA}=[\mathrm{HCO_3^-}]+2[\mathrm{CO_3^{2-}}] \quad (12)$$

The total alkalinity (TA) is defined by (see Zeebe and Wolf-Gladrow, 2003, for more details):

$$\mathrm{TA}=\mathrm{CA}+[\mathrm{B(OH)_4^-}]+[\mathrm{OH^-}]-[\mathrm{H^+}] \quad (13)$$

We denote $\lambda=\mathrm{TA}-2[\mathrm{Ca^{2+}}]=\mathrm{TA}-2S_2$. To a first approximation, the ions that most contribute to λ depend on the salinity and remain constant.

Following the previous considerations, carbonate alkalinity then only depends on calcium: $\mathrm{CA}=\lambda-\lambda_0+2S_2$ (where, to a first approximation, $\lambda_0=[\mathrm{B(OH)_4^-}]+[\mathrm{OH^-}]-[\mathrm{H^+}]$ remains constant compared to CA). In order to compute $[\mathrm{HCO_3^-}]$ and $[\mathrm{CO_3^{2-}}]$, we use the dissociation constants of the carbon dioxide (K_1) and bicarbonate (K_2):

$$K_1=\frac{\mathrm{h}[\mathrm{HCO_3^-}]}{[\mathrm{CO_2}]}\text{ and }K_2=\frac{\mathrm{h}[\mathrm{CO_3^{2-}}]}{[\mathrm{HCO_3^-}]} \quad (14)$$

where h is the proton concentration, $[H^+]$.The total dissolved inorganic carbon (D) is defined as:

$$D=[HCO_3^-]+[CO_3^{2-}]+[CO_2] \quad (15)$$

Note that, in the considered pH range, $[HCO_3^-]>>[CO_3^{2-}]>>[CO_2]$ (see for example Zeebe and Wolf-Gladrow, 2003). It follows that bicarbonate is the main carbon species in the carbonate system:

$$[HCO_3^-] \simeq D \quad (16)$$

and that the carbonates concentration can be deduced from Eqs. (12) and (15):

$$[CO_3^{2-}] \simeq CA - D \quad (17)$$

With this approximation, we can now compute the following ratio: $r=\frac{D}{[CA}$, using Eqs. (12), (15), and (14); r reads:

$$r=\frac{h+K_2+h^2/K_1}{h+2K_2} \quad (18)$$

It follows that h can be computed as a function of r:

$$h=u(r)=\left(-1+r+\sqrt{(1-2r)(1-4K_2/K_1)+r^2}\right)\frac{K_1}{2} \quad (19)$$

Now using Eqs. (14) and (12), we can compute the CO_2 concentration:

$$[CO_2]=\frac{CA}{K_1}\frac{h^2}{h+2K_2}=CA\,v(r)=\psi(S_2, D) \quad (20)$$

This simplified seawater modelling allowed a mathematical analysis of coccolithophorid models (Bernard et al., 2008). However, in the present numerical simulations, we used a more accurate model that does not make any approximation, and

so resolves the exact concentration of the chemical species. The used Matlab code is a supplement to Zeebe and Wolf-Gladrow (2003), modified to account for calcium consumption.

When coupling growth, calcification and inorganic carbon models, we get the models proposed in Bernard et al. (2008) (plus the model where calcite saturation state is the regulating factor). The analysis in Bernard et al. (2008) demonstrated that $\mathcal{M}_p$ models where D_p was either CO_2 or HCO_3^- supported the results of Iglesias-Rodriguez et al. (2008), while models where CO_3^{2-} or Ω was the regulating factor supported the results obtained by Sciandra et al. (2003). To get a qualitative prediction of the experimental results reported by Riebesell et al. (2000), calcification and photosynthesis had to be decoupled, with photosynthesis driven by CO_2 or HCO_3^- and calcification driven by CO_3^{2-} or Ω.

3 Modelling a bloom of *E. huxleyi* in a mixed layer

3.1 Considered simplified physics

In summer, density gradients generated by increasing temperatures lead to water stratification. The surface layer remains mixed over a generally shallow depth. Here we considered a mixed layer depth L of 15 m, and to keep the model as simple as possible we assumed, as in Tyrell and Taylor (1996), an homogeneous distribution. We simulated the growth of coccolithophorids in this mixed layer, as represented in Fig. 1. CO_2 concentration in the water equilibrates with that in the atmosphere, following the difference in concentration between the two compartments and according to the diffusion coefficient K_L.

In the water, CO_2 equilibrates with HCO_3^- and CO_3^{2-}. The CO_2 pool in the water is also affected by the coccolithophorids activity, being fueled by respiration and consumed through the processes of photosynthesis and calcification (see Eq. 4). The model

simulates a nitrate uptake limited by the availability of NO_3 , as illustrated by Eq. (3). NO_3, DIC and Ca^{2+} in the mixed water are replenished from the deeper waters (with an exchange rate K_d) whose concentration are, respectively, $S_{1,0}$, $S_{2,0}$ and D_0. As the water acidity affects the coccoliths persistence, we accounted for a possible dissolution of coccoliths whose rate is dependent upon pH through the calcite saturation state. We assume that this rate can be written as $\frac{K_{\text{diss}}}{\Omega}$, where K_{diss} is the dissolution rate when Ω=1. Settlement of calcite (coccoliths) is represented through $CaCO_3$ sinking below the mixed layer.

3.2 Model equations

Model equations can then be directly deduced from the mass flows (3) and (4). D_p is the regulating factor (among CO_2, HCO_3^-, CO_3^{2-} and Ω) assumed to control both photosynthesis and calcification. The system of equations reads:

$$\dot{S}_1 = K_d(S_{1,0} - S_1) - \rho(S_1)X \tag{21}$$

$$\dot{Q} = \rho(S_1) - \mu(Q, D_p)Q \tag{22}$$

$$\dot{X} = -K_d X + \mu(Q, D_p)X - RX - K_{\text{sed}}X \tag{23}$$

$$\dot{C} = -K_d C + \frac{1-\alpha}{\alpha}\mu(Q, D_p)X - K_{\text{sed}}C - \frac{K_{\text{diss}}}{\Omega}C \tag{24}$$

$$\dot{D} = K_d(D_0 - D) - \frac{1}{\alpha}\mu(Q, D_p)X + RX \tag{25}$$

$$-K_L(\psi(S_2, D) - K_H\, pCO_2) + \frac{K_{\text{diss}}}{\Omega}C \tag{26}$$

$$\dot{S}_2 = K_d(S_{2,0} - S_2) - \frac{1-\alpha}{\alpha}\mu(Q, D_p)X \tag{27}$$

Where K_d is the exchange rate through the thermocline and K_{sed} the sedimentation rate.

The initial conditions have been chosen assuming that coccolithophorids bloom right after a large diatom bloom which reduced the nitrate and inorganic carbon concentrations in the mixed layer (Riebesell et al., 1993). Inspired by the pCO_2 observations during bloom experiments (Keeling et al., 1996; Benthien et al., 2007), we assume that 0.2 mmol.L^{-1} of total inorganic carbon was consumed by the previous bloom. The reference (i.e. before the diatom bloom) dissolved inorganic carbon concentration was computed assuming an equilibrium with the atmosphere.

3.3 Export fluxes computation

The exported carbon flux is computed following two different phases. First, during the bloom, the flux follows the material export to the deep layer, through the processes of sedimentation and exchange through the thermocline. The end of the bloom occurs after 20 days; in this second phase, we assume that an unmodelled process, i.e. a high cell lysis or a predation event, makes *E. huxleyi* disappear within ten days, concomitantly to a high transparent exopolymer particles (TEP) production (Engel et al., 2004; Harlay et al., 2009). We estimated the fraction of exported carbon after from works on the link between primary production and organic export (De La Rocha and Passow, 2007; Boyd and Trull, 2007). Last, representing the export of coccoliths is far from trivial, as this complex phenomenon is neither clearly understood nor quantitatively described yet. The main export mechanism would be related to particles aggregation, mainly fecal pellets, which is also enhanced with TEP abundance (De La Rocha and Passow, 2007; Boyd and Trull, 2007; Harlay et al., 2009). Let us keep in mind that our goal is not to provide an exhaustive description of this mechanism, but to catch the main range of magnitude with our simplified model.

3.3.1 Export carbon computation during the bloom

During *E.huxleyi* growth, the carbon flux is proportional to the material exported to the deep layer. The average exported POC during the 20 days of the bloom can thus be computed as follows:

$$F^1_{POC} = \frac{\eta_1 L}{20} \int_0^{20} (K_d + K_{sed}) X d\tau \quad (28)$$

where η_1 is the fraction of POC which is not locally degraded (De La Rocha and Passow, 2007).

To compute the exported PIC, we refer to the estimate proposed by Ridgwell et al. (2007), assuming that it is related to the POC flux with a carrying capacity of organic aggregates for minerals (Passow and De la Rocha, 2006), and that a fraction, depending on Ω, may be dissolved. The total flux during the 20 days of the bloom then reads (with parameters as in Ridgwell et al., 2007):

$$F^1_{PIC} = \frac{0.044 \eta_1 L}{20} \int_0^{20} (\Omega - 1)^{0.81} (K_d + K_{sed}) X \, d\tau \quad (29)$$

3.3.2 Export carbon computation in the week after the bloom

As the coccolithophorid bloom declines, a high quantity of TEP is produced (Engel et al., 2004; Harlay et al., 2009), which triggers the efficiency of particle coagulation and formation of macroscopic aggregates (Logan et al., 1995; De La Rocha and Passow, 2007; Kahl et al., 2008). We assume that TEP is related to the remaining POC at the final time of the simulation (i.e. when the bloom starts to decline).

The average daily POC flux during the ten days following the bloom is assumed to be a fraction η_2 of the remaining primary production at the end of the bloom:

$$F^2_{POC} = \frac{\eta_2 L}{10} POC(t=20) \quad (30)$$

BGD
6, 5339–5372, 2009

The same expression as Eq. (31) based on the formulation of Ridgwell et al. (2007) is used to compute the exported PIC:

$$F^2_{PIC} = \frac{0.044 \eta_2 L}{10} (\Omega - 1)^{0.81} POC(t=20) \quad (31)$$

4 Model calibration

Depending on the choice of the regulating inorganic carbon variable D_p, four different models result from the different hypotheses as for the mechanisms driving both photosynthesis and calcification. Even if the objective is to sketch a generic bloom of *E.hux*, the models were carefully calibrated using realistic parameter values, as detailed in the following.

Temperature and salinity are 15°C and 35 g/kg^{-1}, respectively. The residence time in the mixed layer is assumed to be 20 days (Schmidt et al., 2002), while the sedimentation rate K_{sed} was computed with the assumption of an average coccoliths sedimentation rate of 0.75 m/day (Gregg and Casey, 2007). The dissolution constant K_{diss} was computed so that the calcite dissolution rate in standard pCO_2 conditions is 0.75 d^{-1} (Oguz and Merico, 2006). The DIC deep concentration is assumed to be related to atmospheric pCO_2, and depending on the considered pCO_2 scenario, three values will be considered, denoted $D_{0,380}$, $D_{0,760}$ and $D_{0,1140}$. The fraction of POC exported to the deep layer during the bloom (η_1=0.3) and the fraction of the remaining POC exported during the declining phase (η_1=0.1) have been calibrated using ranges provided by (Honjo et al., 2008).

The nitrogen uptake rate is derived from Bernard et al. (2008), together with the values of the half saturation constants K_{D_p} (according to Rost and Riebesell, 2004, see Table 3). The light extinction coefficients are computed from Oguz and Merico (2006).

The maximum exponential growth rate under non limiting conditions can be

computed from the maximum hypothetical growth rate (Bernard and Gouzé, 1995):

$$\mu_{\max}(I)=\bar{\mu}(I)\frac{\rho_m}{k_Q\bar{\mu}(I)+\rho_m} \tag{32}$$

and thus we can get $\bar{\mu}(I)$ from $\mu_{\max}(I)$, issued from Gregg and Casey (2007), taking into account our considered values of temperature and half saturation constant for light intensity:

$$\bar{\mu}(I)=\frac{\rho_m\mu_{\max}(I)}{\rho_m-k_Q\mu_{\max}(I)} \tag{33}$$

Models were calibrated in such a way that they all predict the same carbon fluxes in nowadays pCO_2 (380 ppm), on the basis of available experimental results (Bernard et al., 2008). This means that all models predict the same growth rate under non limiting nitrogen conditions, and with CO_2, HCO_3^-, CO_3^{2-} and Ω computed using standard seawater values (Zeebe and Wolf-Gladrow, 2003). In other words, the computed $\bar{\mu}_{D_p}\frac{D_p}{D_p+K_{D_p}}$ all equal each other for any D_p.

Finally, parameter values are presented in Tables 2 and 3.

At this stage, we can remark that models regulated by CO_3^{2-} and Ω present similar behaviours (data not shown). Indeed the simulations show very close predictions that always differ by less than 1%. This fact is consequent to the stability of Ca^{2+} concentration in seawater, which makes Ω proportional to CO_3^{2-} along the simulation. Note that this property is not straightforward for in vitro experiments (especially in batch conditions) where the high biomass level may affect the Ca^{2+} stock, and thus more drastically influence Ω.

In the sequel we will therefore only consider the model in which the calcite saturation state is the regulating factor.

5 Model simulations

5.1 Simulation at nowadays pCO_2

We used each of the three models to simulate a large bloom of *Emiliania huxleyi*. Phytoplankton cells are assumed to grow in a homogeneous layer, where aqueous CO_2 equilibrates with the atmosphere. It takes several weeks to supply inorganic carbon from both atmosphere and the deeper ocean to the cells in the whole mixed layer, and to reconstitute the stock of inorganic carbon depleted by the previous bloom (Fig. 2). The inorganic carbon stock reconstitution is slowed down by the consumption of inorganic carbon by the *E. huxleyi* bloom. As a consequence, during the simulation, CO_3^{2-} and Ω show higher values, while CO_2 and HCO_3^- are lower compared to their respective steady state value. This fact can explain the significantly different behaviours observed between the 3 scenarii (Fig. 4). Indeed, it turns out that because of the high consumption of CO_2 by the blooming biomass, the progressive depletion of inorganic carbon results in a stronger down regulation of growth and calcification in models controlled by CO_2 or HCO_3^-. On the contrary, the models regulated by CO_3^{2-} or Ω are enhanced by the depletion in inorganic carbon. It results that the predicted, fixed carbon during the bloom formation is twofold in the CO_3^{2-} and Ω models compared to the CO_2 model (Fig. 4).

5.2 Simulation with doubled pCO_2

Based on the accumulation rate of CO_2 observed in the atmosphere from the beginning of the industrial era, current models roughly predict a doubling of the partial pressure of the atmospheric CO_2 (pCO_2). Since the atmosphere tends to be in equilibrium with the superficial oceanic layers, changes in atmospheric CO_2 show direct effects on the CO_2 seawater concentration, and consequently on the carbonate system speciation.

Under such conditions of elevated pCO_2, the initial condition of depleted inorganic carbon concentration in the water column, due to the development of the previous

bloom, is still transiently observed and appears more favorable to the CO_3^{2-} and Ω models (Fig. 5). However this tendency does not last, since inorganic carbon rapidly increases as CO_2 in the water equilibrates with the elevated, atmospheric value. After one week, ambient conditions are back to high CO_2 concentrations and then prove to be much more favorable to the CO_2 and HCO_3^- models which are then stimulated and rapidly recover. Yet, important differences appear in the final PIC and POC concentrations, with much higher predicted values in the CO_2 and HCO_3^- models.

5.3 Discussion

As indicated by the coefficients of variation presented in Table 4, all models predict a two-fold difference in the final concentrations under a doubled pCO_2. Here, simulations suggest that a change in pCO_2 will impact bloom formation in the coccolithophorid *E. huxleyi*. Yet, depending on the model, this variation is an increase (see the doubling in PIC in the CO_2 model) or a decrease (see the 45% PIC drop in the CO_3^{2-} model). Hence, simulations also point out striking, two-fold differences in predicted concentrations, depending on the considered regulating factor. That is, the variability in the predicted values, observed between the models, equals or even exceeds that due to the rise in pCO_2. This statement is reinforced when considering a tripling of pCO_2 (see Table 4). This point is absolutely critical as it demonstrates the strong dependence of the model outcome on the initial hypotheses made as for the regulation of photosynthesis and calcification.

Even though schematic and academic, our simulations nevertheless integrate realistic orders of magnitude for the underlying biological processes. The two phenomena, revealed by our simplified approach, are likely to appear when dealing with more realistic and accurate models as well. The tight dependence of the stock and flux predictions on the underlying regulation mechanisms and the paradoxical effect when inorganic carbon is depleted may both strongly affect any modelling prediction. So far, to our knowledge, none of the complex models dealing with coccolithophorids (Tyrell

and Taylor, 1996; Merico et al.; Oguz and Merico, 2006; Gregg and Casey, 2007) integrates an accurate modelling of the biological effect of a pCO_2 change. As stated by Riebesell (2004), it seems impossible at this point to provide any reliable forecast of large-scale and long-term biological responses to global environmental change. Our study should therefore be considered as a methodological approach on a bench model to highlight a phenomenon that will take place in more detailed models (including food web interactions). As more experimental works are needed to unravel the carbon acquisition modes and their regulation in coccolithophorids, prediction statements should be made with caution and discussed in regard to the plausible hypotheses.

Last, another hypothesis was recently brought forward by several authors: the calcification mechanisms also seems to be highly strain dependent (Fabry, 2008; Langer et al., 2009). As an assemblage of various strains (with different carbon acquisition regulation mechanism), a natural population would then show a range of different responses to increases in pCO_2 . To provide an accurate, simulated response to pCO_2 change, a model should then represent each subpopulation, with various responses to carbonate chemistry, so that the resulting overall response reveals to be a combination of the subpopulation behaviours. This approach may however be strongly affected by parameter uncertainties, such as the initial conditions of each subpopulation, that may jeopardize the model conclusions.

6 Conclusions

This study stresses how correct identification of the chemical species that drive(s) calcification and photosynthesis processes is critical to accurate predictions of coccolithophorids blooms and the consequent amount of carbon withdrawn from the atmosphere and trapped into the deep ocean. Model results reveal a striking difference in the predicted biomass increase when the saturation state Ω (or equivalently CO_3^{2-}) is the regulating factor compared to the CO_2 and HCO_3^-models.

This work also points out the transient periods during which the inorganic carbon is

much lower than its value at equilibrium with the atmosphere. During these transient phases, the scenarii in which CO_3^{2-} or Ω regulate calcification and photosynthesis may be strongly advantaged, leading thus to an unexpected effect.

The new model that we presented, in which the calcite saturation state drives calcification, turns out to be plausible alternative explanation to the CO_3^{2-} model. This model assumes that the calcite saturation state, even when higher than 1 (meaning that dissolution rate is low), strongly influences the calcification rate. The simulation results illustrate a property that could have been shown analytically, using similar principles than in Bernard et al. (2008): the Ω follows the CO_3^{2-} model. This model can thus explain the experimental results obtained by Sciandra et al. (2003). In the hypothesis of uncoupled calcification and photosynthesis, if Ω is used to control the calcification rate while the photosynthesis rate is driven by CO_2, then the experimental results of Riebesell et al. (2000) can be reproduced. A detailed validated model may integrate more accurate knowledge, especially for carbon export, but it may also be affected by the same uncertainties that our bench model, thus resulting in highly uncertain predictions of carbon fluxes in the situations of large blooms of coccolithophorids.

Results thus strongly call for further experimental approaches to more formely identify the chemical species that primarily regulate photosynthesis and calcification.

Acknowledgements. The authors benefited from the support of the BOOM project (Biodiversity of Open Ocean Microcalcifiers) funded by the French National Research Agency (ANR), of the European FP7 Integrated Project EPOCA (European Project on Ocean Acidification).

The publication of this article is financed by CNRS-INSU.

References

Benthien, A., Zondervan, I., Engel, A., Hefter, J., Terbüggen, A., and Riebesell, U.: Carbon isotopic fractionation during a mesocosm bloom experiment dominated by *Emiliania huxleyi*: Effects of CO_2 concentration and primary production, Geochim. Cosmochim. Ac., 71, 1528–1541, 2007. 5351

Bernard, O. and Gouzé, J. L.: Transient Behavior of Biological Loop Models, with Application to the Droop Model, Math. Biosci., 127, 19–43, 1995. 5354

Bernard, O., Sciandra, A., and Madani, S.: Multimodel analysis of the response of the coccolithophore *Emiliania huxleyi* to an elevation of pCO_2 under nitrate limitation , Ecol. Model., 211, 324–338, 2008. 5342, 5343, 5344, 5345, 5348, 5349, 5353, 5354, 5358

Berry, L., Taylor, A. R., Lucken, U., Ryan, K. P., and Brownlee, C.: Calcification and inorganic carbon acquisition in coccolithophores., Funct. Plant. Biol., 29, 1–11, 2002. 5341

Boyd, P. and Trull, T.: Understanding the export of biogenic particles in oceanic waters: Is there consensus?, Prog. Oceanogr., 72, 276–312, 2007. 5351

Buitenhuis, E. T., de Baar, H. J. W., and Veldhuis, M. J. V.: Photosynthesis and calcification by *Emiliania huxleyi* (Prymnesiophyceae) as a function of inorganic carbon species., J. Phycol., 35, 949–959, 1999. 5342

Burmaster, D.: The unsteady continuous culture of phosphate-limited *Monochrisis lutheri Droop*: Experimental and theoretical analysis, J. Exp. Mar. Biol. Ecol., 39(2), 167–186, 1979. 5343

De La Rocha, C. and Passow, U.: Factors influencing the sinking of POC and the efficiency of the biological carbon pump, Deep-Sea Res. Pt. II, 54, 639–658, 2007. 5351, 5352

Droop, M. R.: Vitamin B12 and marine ecology. IV. The kinetics of uptake growth and inhibition in *Monochrysis lutheri*, J. Mar. Biol. Assoc. UK, 48, 689–733, 1968. 5343, 5344, 5346

Droop, M. R.: 25 Years of Algal Growth Kinetics, A Personal View, Bot. Mar., 16, 99–112, 1983. 5343, 5344, 5346

Dugdale, R. C.: Nutrient limitation in the sea: dynamics, identification and significance, Limnol. Oceanogr., 12, 685–695, 1967. 5344

Engel, A., Delille, B., Jacquet, S., Riebesell, U., Rochelle-Newall, E., Terbruggen, A., and Zondervan, I.: Transparent exopolymer particles and dissolved organic carbon production by *Emiliania huxleyi* exposed to different CO_2 concentrations: a mesocosm experiment, Aquat. Microb. Ecol., 34, 93–104, 2004. 5351, 5352

Fabry, V. J.: Ocean science – Marine calcifiers in a high-CO_2 ocean, Science, 320, 1020–1022, 2008. 5357
Falkowski, P. G.: Evolution of the nitrogen cycle and its influence on the biological sequestration of $CO_2$2 in the ocean, Nature, 327, 242–244, 1997. 5341
Frankignoulle, M., Canon, C., and Gattuso, J. P.: Marine calcification as a source of carbon dioxide: positive feedback of increasing atmospheric CO_2, Limnol. Oceanogr., 39, 458–462, 1994. 5340
Gregg, W. W. and Casey, N. W.: Modeling coccolithophores in the global oceans, Deep-Sea Res. Pt. II, 54, 447–477, 2007. 5353, 5354, 5357
Harlay, J., Bodt, C. D., Engel, A., Jansen, S., d'Hoop, Q., Piontek, J., Oostende, N. V., Groom, S., Sabbe, K., and Chou, L.: Abundance and size distribution of transparent exopolymer particles (TEP) in a coccolithophorid bloom in the northern Bay of Biscay, Deep-Sea Res. Pt. I, in press, 2009. 5351, 5352
Honjo, S., Manganini, S. J., Krishfield, R. A., and Francois, R.: Particulate organic carbon fluxes to the ocean interior and factors controlling the biological pump: a synthesis of global sediment trap programs since 1983, Prog. Oceanogr., 76, 217–285, 2008. 5353
Houghton, J. T., Jenkins, G. J., and Ephtraims, J. J.: Climate Change 1995, The Science of Climate Change, Cambridge University Press, Cambridge, 572 pp., UK, 1996. 5341
Iglesias-Rodriguez, M. D., Halloran, P. R., Rickaby, R. E. M., Hall, I. R., Colmenero-Hidalgo, E., Gittins, J. R., Green, D. R. H., Tyrrell, T., Gibbs, S. J., von Dassow, P., Rehm, E., Armbrust, E. V., and Boessenkool, K. P.: Phytoplankton Calcification in a High-CO_{22} World, Science, 320, 336–340, 2008. 5341, 5349
Kahl, L., Vardi, A., and Schofield, O.: Effects of phytoplankton physiology on export flux, Mar. Ecol.-Prog. Ser., 354, 3–19, 2008. 5352
Keeling, R. F., Piper, S. C., and Heimann, M.: Global and hemispheric $CO_2$2 sinks deduced from changes in atmospheric O2 concentration, Nature, 381, 308–341, 1996. 5351
Klepper, O., de Haan, B. J., and van Huet, H.: Biochemical feedbacks in the oceanic carbon cycle, Ecol. Model., 75, 459–469, 1994. 5341
Langer, G., Nehrke, G., Probert, I., Ly, J., and Ziveri, P.: Strain-specific responses of Emiliania huxleyi to changing seawater carbonate chemistry, Biogeosciences Discuss., 6, 4361–4383, 2009, http://www.biogeosciences-discuss.net/6/4361/2009/. 5357
Leonardos, N. and Geider, R. J.: Elemental and biochemical composition of Rhodomonas

reticulata (Cryptophyta) in relation to light and nitrate-to-phosphate supply ratios, J. Phycol., 41, 567–576, 2005. 5341

Logan, B. E., Passow, U., Alldredge, A. L., Grossartt, H.-P., and Simont, M.: Rapid formation and sedimentation of large aggregates is predictable from coagulation rates (half-lives) of transparent exopolymer particles (TEP), Deep-Sea Res. Pt. II, 42, 203–214, 1995. 5352

Merico, A., Tyrrell, T., Lessard, E., Oguz, T., Stabeno, P., Zeeman, S., and Whitledge, T.: Modelling phytoplankton succession on the Bering Sea shelf: role of climate influences and trophic interactions in generating Emiliania huxleyi blooms 1997–2000, Deep-Sea Res. Pt. I, 51, 1803–1826, 2004. 5357

Merico, A., Tyrrell, T., and Cokacar, T.: Is there any relationship between phytoplankton seasonal dynamics and the carbonate system?, J. Mar. Syst., 59, 120–142, 2006. 5342

Millero, F.: The Marine Inorganic Carbon Cycle, Chem. Rev., 107, 308–341, 2007. 5347

Nimer, N. and Merrett, M.: Calcification rate in *Emiliania huxleyi* Lohmann in response to light, nitrate and availability of inorganic carbon, New Phytol., 123, 673–677, 1993. 5346

Nimer, N. A. and Merrett, M. J.: The development of a CO_2-concentrating mechanism in *Emiliania huxleyi*., New Phytol., 133, 387–389, 1996. 5342

Oguz, T. and Merico, A.: Factors controlling the summer *Emiliania huxleyi* bloom in the Black Sea: A modeling study, J. Marine Syst., 59, 173–188, 2006. 5346, 5353, 5357

Orr, J., Fabry, V., Aumont, O., Bopp, L., Doney, S., Feely, R., Gnanadesikan, A., Gruber, N., Ishida, A., Joos, F., Key, R., Lindsay, K., Maier-Reimer, E., Matear, R., Monfray, P., Mouchet, A., Najjar, R., Plattner, G., Rodgers, K., Sabine, C., Sarmiento, J., Schlitzer, R., Slater, R., Totterdell, I., Weirig, M., Yamanaka, Y., and Yool, A.: Anthropogenic ocean acidification over the twenty-first century and its impact on calcifying organisms, Nature, 437, 681–686, 2005. 5341

Paasche, E.: A tracer study of the inorganic carbon uptake during coccolith formation and photosynthesis in the coccolithophorid *Coccolithus huxleyi*., Physiol. Plantarum., 3, 1–82, 1968. 5341

Paasche, E.: A review of the coccolithophorid *Emiliania huxleyi* (Prymnesiophyceae), with particular reference to growth, coccolith formation, and calcification-photosynthesis interaction, Phycologia, 40, 503–529, 2002. 5341

Passow, U. and De la Rocha, C.: Accumulation of mineral ballast on organic aggregates, Global Biogeochem. Cy., 20, GB1013, 2006. 5352

Ridgwell, A., Zondervan, I., Hargreaves, J. C., Bijma, J., and Lenton, T. M.: Assessing the

potential long-term increase of oceanic fossil fuel CO_{22} uptake due to CO_{22}-calcification feedback, Biogeosciences, 4, 481–492, 2007, http://www.biogeosciences.net/4/481/2007/. 5352, 5353

Riebesell, U.: Effects of CO_{22} Enrichment on Marine Phytoplankton, J. Oceanogr., 60, 719–729, 2004. 5342, 5357

Riebesell, U., Zondervan, I., Rost, B., Tortell, P., Zeebe, R. E., and Morel, F. M. M.: Reduced calcification of marine plankton in response to increased atmospheric CO_2, Nature, 407, 364–367, 2000. 5341, 5342, 5349, 5358

Riebesell, U., Wolf-Gladrow, A., and Smetacek, V.: Carbon dioxide limitation of marine phytoplankton growth rates , Science, 361, 249–251, 1993. 5343, 5351

Riebesell, U., Bellerby, R. G. J., Engel, A., Fabry, V. J., Hutchins, D. A., Reusch, T. B. H., Schulz, K. G., and Morel, F. M. M.: Comment on "Phytoplankton Calcification in a High-CO_2 World", Science, 322, 1466 pp., 2008. 5341

Rost, B. and Riebesell, U.: Coccolithophores and the biological pump: responses to environmental changes, in: Coccolithophores. From Molecular Processes to Global Impact, edited by: Thierstein, H. R. and Young, J. R., Springer, Berlin, Germany, 99–127, 2004. 5353

Rost, B., Riebesell, U., Burkhardt, S., and Sultemeyer, D.: Carbon acquisition of bloom-forming marine phytoplankton., Limnol. Oceanogr., 48, 44–67, 2003. 5342

Rost, B., Riebesell, U., and Sultemeyer, D.: Carbon acquisition of marine phytoplankton: Effect of photoperiod length, Limnol. Oceanogr., 51, 12–20, 2006. 5342

Schmidt, S., Chou, L., and Hall, I.: Particle residence times in surface waters over the North-Western Iberian Margin: comparison of pre-upwelling and winter periods, J. Marine. Syst., 32, 3–11, 2002. 5353

Sciandra, A., Harlay, J., Lefévre, D., Lemée, R., Rimmelin, P., Denis, M., and Gattuso, J.-P.: Response of coccolithophorid *Emiliania huxleyi* to elevated partial pressure of CO_2 under nitrogen limitation., Mar. Ecol. Prog. Ser., 261, 111–122, 2003. 5341, 5342, 5349, 5358

Tyrell, T. and Taylor, A.: A modelling study of *Emiliania huxleyi* in the NE Atlantic , J. Marine. Syst., 9, 83–112, 1996. 5349, 5356

Zeebe, R. E. and Wolf-Gladrow, D.: CO_2 in seawater: equilibrium, kinetics, isotopes, Elsevier, 2001 pp., 2003.

5347, 5348, 5349, 5354

Table 1. Definition of variables and fluxes for the four considered models .

	Meaning	Unit
D	Dissolved inorganic carbon (DIC)	$mmol.L^{-1}$
N	Particulate nitrogen (PON)	$mmol.L^{-1}$
Q	Internal nitrogen quota	$mmol\,N.(mmol\,C)^{-1}$
X	Particulate organic carbon (POC)	$mmol.L^{-1}$
C	Coccoliths concentration (PIC)	$mmol.L^{-1}$
S_1	Nitrate	$mmol.L^{-1}$
S_2	Calcium	$mmol.L^{-1}$
Ω	Calcite saturation state	–
F^1_{POC}	POC flux during growth phase	$mmol\,C.day^{-1}.m^{-2}$
F^1_{PIC}	PIC flux during growth phase	$mmol\,C.day^{-1}.m^{-2}$
F^2_{POC}	POC flux during decay phase	$mmol\,C.day^{-1}.m^{-2}$
F^2_{PIC}	PIC flux during decay phase	$mmol\,C.day^{-1}.m^{-2}$

BGD
6, 5339–5372, 2009

Table 2. Definitions and values of the model parameters. [1]: depends on the model type, see Table 3. [†]: unitless for Ω.

	Value	Meaning
α	0.53 –	proportion of DIC for photosynthesis
η_1	0.3 –	fraction of exported POC flux
η_2	0.1 –	fraction of exported POC
μ	. d^{-1}	photosynthesis rate
$\bar{\mu}$	.[1] d^{-1}	max. hypothetical photosynthesis rate
ρ	. μmol N.mmol C^{-1}.d^{-1}	NO_3 uptake rate
ρ_m	100.19 μmol N.mmol C^{-1}.d^{-1}	maximum NO_3 uptake rate
$D_{0,380}$	2.07 mmol C.L^{-}1	DIC deep concentration
$D_{0,760}$	2.18 mmol $C.L^{-1}$	DIC deep concentration
I_0	300 μmol $Q.m^{-2}.s^{-1}$	mean incident light
k_1	0.07 m^{-1}	light extinction rate
k_2	0.05 m^{-1}.mmolN^{-1}	light extinction rate
k_{D_p}	.[1] μmol.L^{-1}†	affinity constant for D_p
k_N	0.038 μmol.L^{-1}	affinity constant for NO_3
k_Q	32.29 μmol N.mmol C^{-1}	internal subsistance quota
K_1	1.392 10^{-6} mol.L^{-1}	equilibrium constant
K_2	1.189 10^{-9} mol.L^{-1}	equilibrium constant
K_{diss}	0.16 d^{-1}	coccolith dissolution rate for Ω=1
K_d	0.05 d^{-1}	exchange rate through thermocline
K_H	36.7 mmol $CO_{22}.L^{-1}.\mu$atm	Henry's constant
K_I	50 μmol$Q.m^{-2}.s^{-1}$	affinity constant for light
K_L	5.87 dm.d^{-1}	CO_2 transfer coefficient
K_{sed}	0.05 d^{-1}	sedimentation rate
L	15 m	mixed layer depth
R	0.05 d^{-1}	respiration rate
$S_{1,0}$	5 μmol $N.L^{-1}$	NO_3 deep concentration
$S_{2,0}$	10.4 mmol $Ca.L^{-1}$	Ca deep concentration
z	. m	depth

BGD
6, 5339–5372, 2009

Table 3. Kinetics parameters depending on the chosen model (†: unitless for k_{Ω})

.

Parameters	CO_3^{2-}	HCO_3^-	CO_2	Ω	Units
k_{D_p}	0.076	1.65	0.015	$3.23^{\dagger}$	μmol C.L^{-1}
$\bar{\mu}$	1.34	0.96	1.7	1.64	d^{-1}

Table 4. Final values of PIC and POC at t=20 days, and average dayly exported carbon during the bloom, in mg C.m^{-2}.d^{-1} with respect to the considered model and pCO_2. CV: coefficient of variation (expressed in %).

	pCO_2 (ppm)	$\mathcal{M}$ CO_2	$\mathcal{M}$ HCO_3^-	$\mathcal{M}$ Ω	CV/$\mathcal{M}$ (%)
PIC	380	238.93	350.91	575.25	44.10
(t=20)	760	467.66	350.21	256.47	29.55
μg/l	1140	670.82	317.81	128.00	74.01
CV(%)		*47.06*	*5.57*	*71.98*	
POC	380	262.58	383.57	631.62	44.17
(t=20)	760	585.64	441.80	326.96	28.71
μg/l	1140	981.56	470.93	199.90	72.06
CV(%)		*59.04*	*10.29*	*57.45*	
F_{PIC}	380	13.97	20.41	33.58	44.14
$+F_{POC}$	760	30.65	23.14	17.14	28.62
mg/m^2/d	1140	50.38	24.32	10.36	71.64
CV(%)		*57.57*	*8.87*	*58.65*	

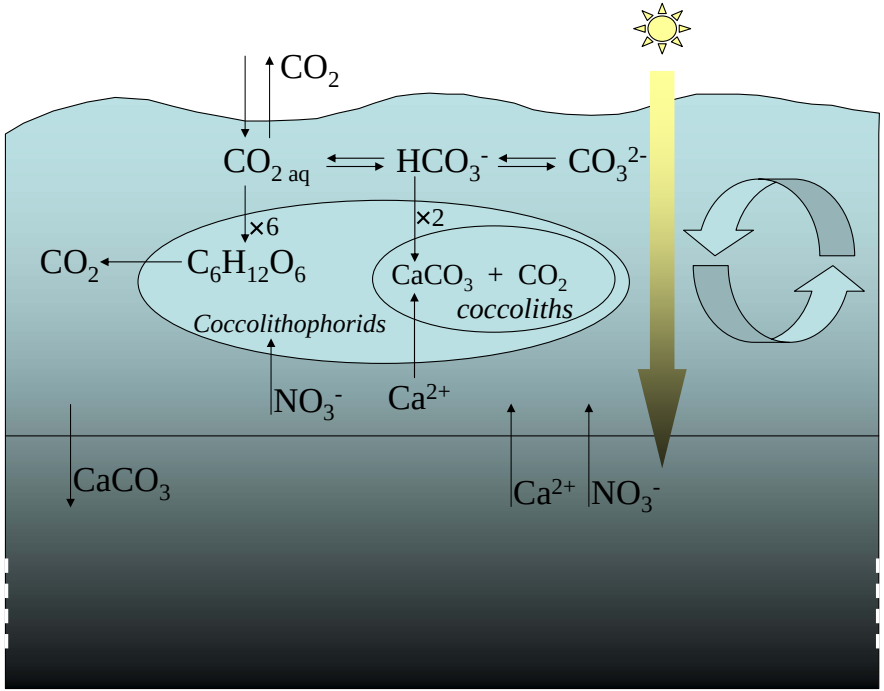

Fig. 1. Schematic diagram of the well mixed upper ocean represented by the model.

BGD
6, 5339–5372, 2009

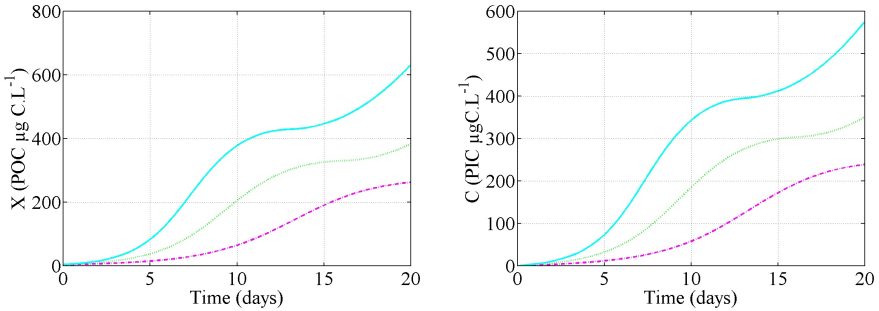

Fig. 2. Simulated PIC and POC at pCO_2=380 ppm with the three models differing by the considered regulating variable D_p (CO_2: _ , HCO_3^-: . . . and Ω: _).

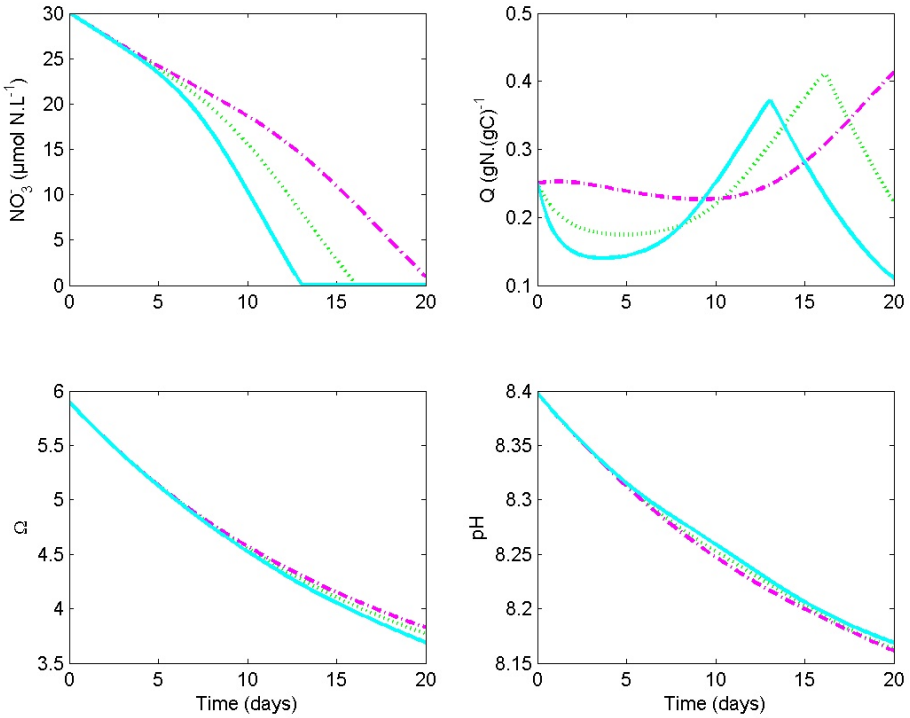

Fig. 3. Simulated nitrate concentration, internal quota, calcite saturation state and pH, depending on the considered regulating variable D_p (CO_2: - . - , HCO_3^-: . . . and Ω: – –) pCO_2=380 ppm.

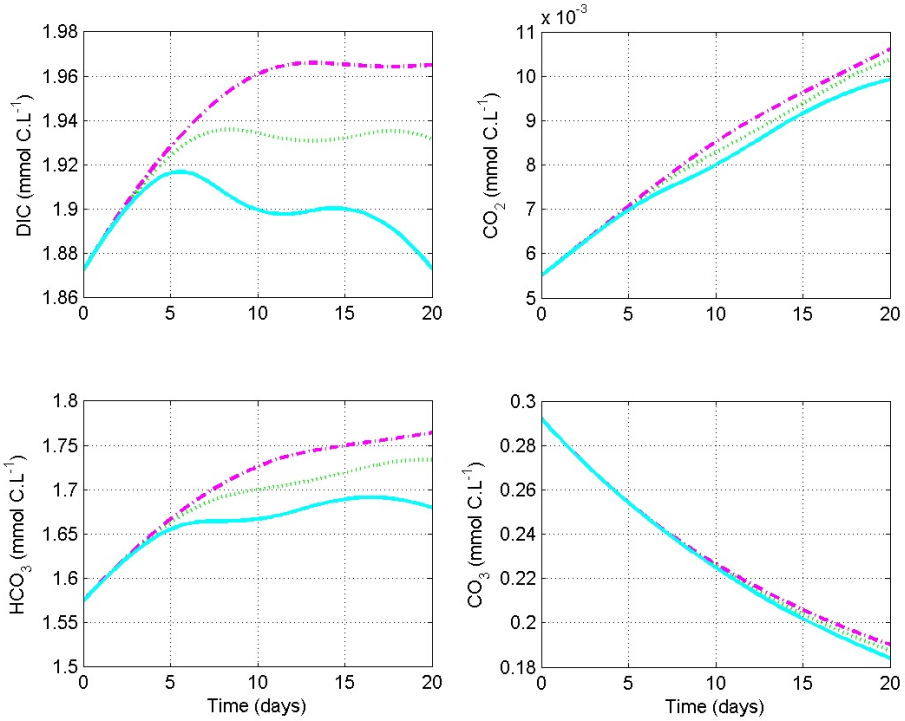

Fig. 4. Simulated inorganic carbon with the three models at pCO_2=380 ppm differing by the considered regulating variable D_p (CO_2: _ . _ , HCO_3^-: . . . and Ω: _ _).

BGD
6, 5339–5372, 2009

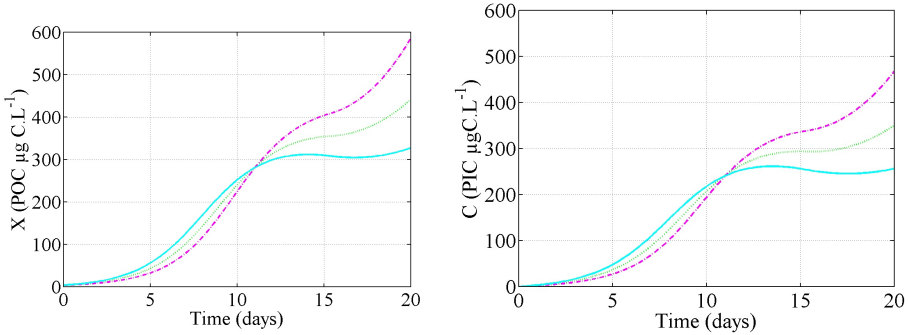

Fig. 5. Simulated PIC and POC at pCO_2=760 ppm with the three models differing by the considered regulating variable D_p(CO_2: _ _ , HCO_3^-:. . . and Ω: __).

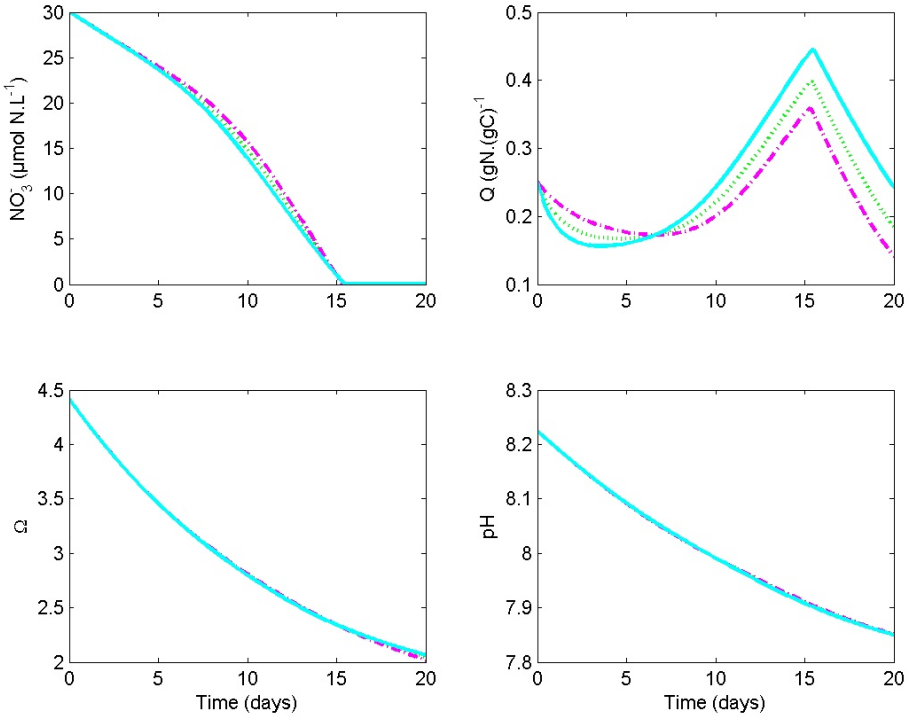

Fig. 6. Simulated nitrate concentration, internal quota, calcite saturation state and pH, depending on the considered regulating variable D_p (CO_2: - - , HCO_3^-: . . . and Ω: _ _). pCO_2=760 ppm.

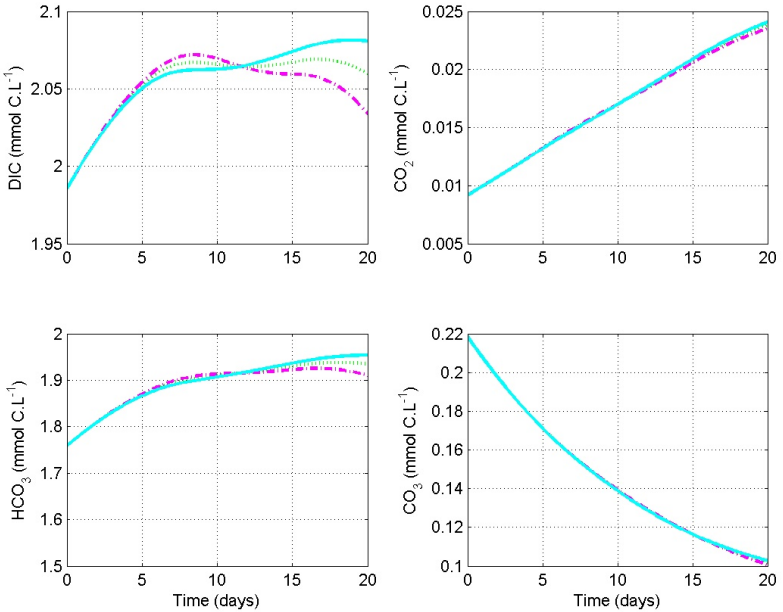

Fig. 7. Simulated inorganic carbon with the three models at pCO_2=760 ppm differing by the considered regulating variable D_p (CO_2: - - , HCO_3^-: . . . and Ω: –).

BGD
6, 5339–5372, 2009

Title Page
Abstract | Introduction
Conclusions | References
Tables | Figures
◀| |▶
◀ ▶
Back | Close
Full Screen / Esc
Printer-friendly Version
Interactive Discussion